Working Report 98-17e

Posiva's site investigations in Olkiluoto, Kivetty, Romuvaara and Hästholmen by He-gas methods in 1997

Kari Hartikainen

Juhani Hartikainen

February 1998

POSIVA OY
Mikonkatu 15 A, FIN-00100 HELSINKI, FINLAND
Tel. +358-9-2280 30
Fax +358-9-2280 3719

Working Report 98-17e

Posiva's site investigations in Olkiluoto, Kivetty, Romuvaara and Hästholmen by He-gas methods in 1997

Kari Hartikainen

Juhani Hartikainen

Oy Helium Gas Research HGR Ltd

February 1998

Working Report 98-17e

Posiva's site investigations in Olkiluoto, Kivetty, Romuvaara and Hästholmen by He-gas methods in 1997

Kari Hartikainen

Juhani Hartikainen

February 1998

TEKIJÄORGANISAATIO: Oy Helium Gas Research HGR Ltd
Kekkolantie 25 A
40520 JYVÄSKYLÄ

TILAAJA: Posiva Oy
Mikonkatu 15 A
00100 HELSINKI

TILAUSNUMERO: 95026/97/AJH

POSIVAN TARKASTAJA:

POSIVAN HYVÄKSYJÄ:

KONSULTIN YHTEYSHENKILÖ: Tj Kari Hartikainen Oy HGR Ltd

TYÖRAPORTTI 98-17

LOPPUSIJOITUSPAIKKAVAIHTOEHTOJEN KALLIOPERÄNÄYTTEIDEN MITTAUKSET He-KAASUMENETELMÄLLÄ STATISTIIKAN LISÄÄMISEKSI

TEKIJÄT: Kari Hartikainen, FM
Juhani Hartikainen, FM

TARKASTAJA JA HYVÄKSYJÄ: Kari Hartikainen
Toimitusjohtaja

POSIVA'S SITE INVESTIGATIONS IN OLKILUOTO, KIVETTY, ROMUVAARA AND HÄSTHOLMEN BY He-GAS METHODS IN 1997

ABSTRACT

The main goal of this study was to produce more statistics for porosity and migration properties of rock samples from Olkiluoto, Kivetty and Romuvaara by He-gas methods. The second goal of this study was to start to produce the corresponding data from a new repository site candidate Hästholmen, situated in Loviisa. The third goal of this study was to test the correspondence between through-diffusion and channel-flow methods.

20 short and 24 long drill core samples from Posiva's site investigations in Olkiluoto, Kivetty, Romuvaara and Hästholmen were measured. Short drill core samples were measured by the helium gas through-diffusion and permeability methods, and long drill core samples by the channel-flow method (Väätäinen et al. 1993, Hartikainen et al. 1994a, Hartikainen et al. 1994b, Hartikainen et al. 1995a, Hartikainen et al. 1995b, Hartikainen et al. 1996a and Hartikainen et al. 1996b). The through-diffusion method was used to determine the porosities and effective diffusion coefficients of the short drill core samples, and the permeability measurements of their permeability coefficients. The channel-flow method was used to determine the products of porosity and effective diffusion coefficient of the long drill core samples. The matrix porosities and effective diffusion coefficients are for helium in samples saturated with nitrogen gas.

The measured through-diffusion porosities varied between 0.04 and 0.20 % and the effective diffusion coefficients of helium in samples saturated by nitrogen gas between 4.30×10^{-10} and 1.85×10^{-8} m^2/s. The measured permeability coefficients varied between 4.0×10^{-20} and 1.5×10^{-17} m^2. The products of porosity and effective diffusion coefficient measured by the through-diffusion method varied between 2.65×10^{-13} and 3.70×10^{-11} m^2/s and measured by the channel-flow method varied between 2.0×10^{-16} and 2.0×10^{-13} m^2/s.

The results from the channel-flow measurements were in each case smaller than the corresponding results obtained from the through-diffusion measurements. This difference is significant if the product ($\varepsilon_p \times D_e$) for through-diffusion result is about 10^{-11} m^2/s. This indicates both that there can be microcracks in these rock types and that the through-diffusion measuring times are short ones (under 500 minutes). The mathematical model for channel-flow measurements does not observe that helium penetrates through the long drill core samples in radial direction during the measurements and the fitted channel-flow results can be wrong (about 10^{-16} m^2/s, should be about 10^{-11} m^2/s). If the determined channel-flow result for the product ($\varepsilon_p \times D_e$) is about 10^{-16} m^2/s, the through-diffusion measurement has to be made for the short drill core sample cut from the long drill core sample to verify the consistency of results. Furthermore, the results show that there are significant variations in the rock characteristics, even within a given rock type from one site. Moreover, there was a close correspondence between the effective diffusion coefficient and permeability coefficient results. This indicates that the effective diffusion and permeability coefficients strongly correlate with each other. It is also worth noting that there was one short drill core sample impermeable to gas (both in the through-diffusion and the permeability measurements). This sample was impermeable even under a pressure difference of about 100 kPa.

In this study the He-gas methods were used for the first time to measure migration properties on the samples from Hästholmen. On the basis of rather limited number of samples, the determined results from Hästholmen were found to be very comparable to the results from the other three possible repository sites.

Keywords: He-gas method, through-diffusion method, permeability method, channel-flow method, porosity, effective diffusion coefficient, permeability coefficient

POSIVAN LOPPUSIJOITUSPAIKKAVAIHTOJEN KALLIOPERÄNÄYTE-TUTKIMUKSIA He-KAASUMENETELMÄLLÄ VUODEN 1997 AIKANA

TIIVISTELMÄ

He-kaasumenetelmällä mitattiin kivinäytteiden huokoisuus- ja kulkeutumisominaisuuksia kolmesta loppusijoituspaikkavaihtoehdosta, Olkiluodosta, Kivetystä ja Romuvaarasta statistiikan lisäämiseksi. Lisäksi mitattiin vastaavia alustavia kulkeutumisparametrituloksia neljännestä loppusijoituspaikkavaihtoehdosta, Loviisan Hästholmenista. Edelleen verrattiin läpidiffuusio- ja kanavamittausmenetelmällä saatuja tuloksia keskenään.

Työssä tutkittiin yhteensä 20 lyhyttä läpidiffuusionäytettä ja 24 pitkää tankokivinäytettä Posiva Oy:n tutkimuspaikkakunnilta Olkiluodosta, Kivetystä, Romuvaarasta ja Hästholmenista. Lyhyet läpidiffuusionäytteet mitattiin sekä läpidiffuusio- että permeabiliteettimenetelmillä ja pitkät tankokivinäytteet kanavamittausmenetelmällä (Väätäinen et al. 1993, Hartikainen et al. 1994a, Hartikainen et al. 1994b, Hartikainen et al. 1995a, Hartikainen et al. 1995b, Hartikainen et al. 1996a ja Hartikainen et al. 1996b). Läpidiffuusiomittauksilla saatiin määritettyä näytteiden huokoisuudet ja efektiiviset diffuusiokertoimet. Permeabiliteettimittauksista saatiin vastaavasti selville näytteiden permeabiliteettikertoimet. Kanavamittauksista saatiin selville huokoisuuksien ja efektiivisten diffuusiokertoimien tulot tankokivinäytteille. Kaasufaasissa mitatut matriisi-huokoisuudet ja efektiiviset diffuusiokertoimet määritettiin heliumin avulla näytteille, joiden huokoset olivat saturoituneet kaasumaisella typellä.

Läpidiffuusiomenetelmällä määritetyt huokoisuudet vaihtelivat välillä 0.04 ja 0.20 % ja efektiiviset diffuusiokertoimet välillä 4.30×10^{-10} ja 1.85×10^{-8} m^2/s. Permeabiliteettikertoimet vaihtelivat vastaavasti välillä 4.0×10^{-20} ja 1.5×10^{-17} m^2. Läpidiffuusiomittauksista määritetyt huokoisuuksien ja efektiivisten diffuusiokertoimien tulot vaihtelivat välillä 2.65×10^{-13} ja 3.70×10^{-11} m^2/s. Vastaavasti kanavamittauksista määritetyt huokoisuuksien ja efektiivisten diffuusiokertoimien tulot vaihtelivat välillä 2.0×10^{-16} ja 2.0×10^{-13} m^2/s.

Tulokset osoittivat, että kanavamittaustulokset olivat säännöllisesti pienempiä kuin vastaavat läpidiffuusiomittaustulokset. Ero oli merkittävä niissä tapauksissa, joissa läpidiffuusio-mittauksista määritetty huokoisuuden ja efektiivisen diffuusiokertoimen tulo oli suuruusluokkaa 10^{-11} m^2/s. Syynä tulosten eroavuuksiin olivat sekä eri kivilajien erilaiset rakenteet, lähinnä mahdollinen mikrorakoilu, että läpidiffuusiomittausten lyhyet mittausajat (kokonaismittausaika yleensä alle 500 minuuttia). Kanavamittauksissa käytetty matemaattinen malli ei ota huomioon heliumin mahdollista tunkeutumista näytteen läpi radiaalisuunnassa kanavamittauksen aikana. Jos helium tunkeutuu näytteen läpi kanavamittauksissa mittausaikana, tuloksiin tulee suhtautua varauksellisesti ja esimerkiksi tulo 10^{-16} m^2/s voi olla suuruusluokkaa 10^{-11} m^2/s. Kyseisissä tapauksissa tankonäytteistä tulee sahata läpidiffuusionäytteitä ja varmistaa niiden avulla tulosten konsistenttius. Lisäksi tulokset osoittivat, että jopa saman kivilajin sisällä tuloksissa oli merkittäviä eroja. Efektiivisien diffuusiokertoimien ja permeabiliteettikertoimien välillä näytti sen sijaan olevan vahva korrelaatio. Yksi läpidiffuusionäyte oli lisäksi läpäisemätön niin läpidiffuusio- kuin permeabiliteettimittauksissa useista toistokokeista huolimatta. Näyte ei läpäissyt merkkiainetta edes 100 kPa:n paine-erolla.

Tässä työssä sovellettiin ensimmäistä kertaa He-kaasumittausmenetelmää joukolle Hästholmenin kivinäytteitä kulkeutumisominaisuuksien määrittämiseksi. Alustavat tulokset osoittivat, että Hästholmenin kivilajit ovat kulkeutumisominaisuuksiltaan hyvin samankaltaisia muiden loppusijoituspaikkavaihtoehtojen kivilajien kanssa He-kaasumenetelmällä määritettynä.

Avainsanat: He-kaasumenetelmä, läpidiffuusiomenetelmä, permeabiliteettimenetelmä, kanavamittausmenetelmä, huokoisuus, efektiivinen diffuusiokerroin, permeabiliteettikerroin

TABLE OF CONTENTS

SYMBOLS

Symbol	Quantity	Unit
ε_p	porosity	[%]
D_e	effective diffusion coefficient	[m^2/s]
K	permeability coefficient	[m^2]

1 INTRODUCTION

Porosities and migration properties of several types of rock from Posiva's site investigations in Olkiluoto, Kivetty and Romuvaara have been measured by He-gas methods during 1996 (Hartikainen et al. 1997). These measurements and the variations of the determined results have shown that much more statistics is needed. In this study a collection of short and long drill core samples from Posiva's site investigations in Olkiluoto, Kivetty, Romuvaara and Hästholmen were measured and analysed. These series of measurements make it possible to complement the data, which will be utilised to compare variations in the rock characteristics of the four possible repository sites. For the same purpose, it is also useful to compare the results between through-diffusion and channel-flow methods. The main purpose of this study is both to get more representative values for the bedrock characteristics of these sites and to test the correspondence between through-diffusion and channel-flow methods. Finally, the permeability measurements are made to verify the correspondence between the effective diffusion coefficient and permeability coefficient results.

Six short and six long drill core samples from both Olkiluoto and Romuvaara (three types of rock), four short and four long drill core samples from Kivetty (two types of rock), and four short and eight long drill core samples from Hästholmen (one type of rock) were measured. In all, 44 samples were measured, consisting of 20 short and 24 long drill cores.

2 SAMPLES

Before the measurements, all short drill core samples were dried from 4 to 21 hours in a vacuum chamber at room temperature. The diameters of the samples varied between 40.6 and 41.8 mm and their lengths between 19.9 and 21.2 mm. These thin samples were cut out from the ends of the long drill core samples.

Correspondingly, before the measurements, all long drill core samples were dried from 4 to 53 hours in a vacuum chamber at room temperature. The diameters of the long drill core samples varied between 40.6 and 41.8 mm (as in case of short drill core samples) and their lengths varied between 404 and 919 mm.

3 MEASUREMENTS AND ANALYSES

The short drill core samples were measured first by the through-diffusion and permeability methods. The through-diffusion and permeability measurements were made by using the standard methods described in detail in our previous reports (Väätäinen et al. 1993, Hartikainen et al. 1994a, Hartikainen et al. 1994b, Hartikainen et al. 1995a, Hartikainen et al. 1995b, Hartikainen et al. 1996a and Hartikainen et al. 1996b).

Secondly, the long drill core samples were measured by the channel-flow method with several flow rates. The channel-flow measurements were also made by the methods previously described. The flow rates that were used in the measurements varied between (2 – 200)$\times 10^{-8}$ m^3/s. The aperture of the channel was about 0.2 mm, its inner diameter was about 41.7 mm, and its length varied between 452 and 967 mm.

The whole break-through diffusion curves and permeability data with several pressure differences ((15-160) kPa) were measured for 20 short drill core samples and the results fitted by mathematical models. These fits were used to determine the matrix porosities, the effective diffusion coefficients of helium in samples saturated with nitrogen gas, and their permeability coefficients. Channel-flow measurements were made for 24 original long drill core samples and for one sample, which was put together with two original samples. Hydrodynamic dispersion, molecular diffusion and matrix diffusion were included in the model calculations used to fit the whole break-through curves measured by the channel-flow for different flow rates. As a result from the these fits, the products of matrix porosities and effective diffusion coefficients of helium in samples saturated with nitrogen gas were determined.

4 RESULTS

The porosities measured by through-diffusion varied between 0.040 and 0.20 %, and the effective diffusion coefficients of helium in samples saturated by nitrogen gas between 4.30×10^{-10} and 1.85×10^{-8} m^2/s. The measured permeability coefficients varied between 4.0×10^{-20} and 1.5×10^{-17} m^2. The products of matrix porosities and effective diffusion coefficients of helium in samples saturated with nitrogen gas varied from 2.65×10^{-13} to

3.70×10^{-11} m^2/s (through-diffusion) and from 2.0×10^{-16} to 2.0×10^{-13} m^2/s (channel-flow). All the results are shown in detail in Table 1. The measured break-through curves and the corresponding results of the model calculations are shown in Appendix A. Similarly, the results of channel-flow measurements are shown in Appendix B.

Table 1. *Porosities, effective diffusion coefficients and permeability coefficients of the through-diffusion, permeability and channel-flow samples from Olkiluoto, Kivetty, Romuvaara and Hästholmen. Diffusion coefficients are for helium in samples saturated by nitrogen gas ($D_e(He/N_2)$).*

Sample	Rock type	Permeability K	Through-diffusion ε_p	D_e	$\varepsilon_p \times D_e$	Channel-flow $\varepsilon_p \times D_e$
		[m^2]	[%]	[m^2/s]	[m^2/s]	[m^2/s]
OLKILUOTO						
OL5A1	Granite	1.0×10^{-18}	0.175	4.70×10^{-9}	8.23×10^{-12}	9.0×10^{-15}
OL5F1	Granite	1.0×10^{-17}	0.20	1.85×10^{-8}	3.70×10^{-11}	1.0×10^{-15}
OL5E1	Mica gneiss	1.0×10^{-19}	0.17	1.50×10^{-9}	2.55×10^{-12}	1.0×10^{-14}
OL5G1	Mica gneiss	4.0×10^{-20}	0.053	5.00×10^{-10}	2.65×10^{-13}	4.0×10^{-14}
OL5B1	Tonalite	2.0×10^{-18}	0.04	2.80×10^{-9}	1.12×10^{-12}	1.0×10^{-14}
OL5I1	Tonalite	2.0×10^{-19}	0.17	1.23×10^{-9}	2.09×10^{-12}	1.0×10^{-14}
KIVETTY						
Ki3B1	Porphyritic granodiorite	8.0×10^{-19}	0.10	3.60×10^{-9}	3.60×10^{-12}	5.0×10^{-15}
Ki3C1	Porphyritic granodiorite	2.0×10^{-19}	0.063	1.38×10^{-9}	8.69×10^{-13}	5.0×10^{-15}
Ki3D1	Porphyritic granite	1.0×10^{-18}	0.16	8.05×10^{-9}	1.29×10^{-11}	8.0×10^{-16}
Ki3E1	Porphyritic granite	4.0×10^{-18}	0.19	1.67×10^{-8}	3.17×10^{-11}	1.0×10^{-15}
ROMUVAARA						
RO2A1	Leukotonalite (gneiss)	1.3×10^{-19}	0.12	1.13×10^{-9}	1.36×10^{-12}	4.5×10^{-15}
RO2C1	Leukotonalite (gneiss)	1.3×10^{-18}	0.19	8.50×10^{-9}	1.62×10^{-11}	7.0×10^{-15}
RO2J1	Amfibolite (A)	5.0×10^{-20}	0.065	4.30×10^{-10}	2.80×10^{-13}	4.0×10^{-14}
RO2K2	Amfibolite (B)	4.0×10^{-19}	0.14	1.88×10^{-9}	2.63×10^{-12}	2.0×10^{-13}
RO2JK	Amfibolite (A+B)					4.0×10^{-15}
RO2M1	Granodiorite	8.8×10^{-19}	0.18	9.00×10^{-9}	1.62×10^{-11}	6.0×10^{-15}
RO2O2	Granodiorite	-	-	-	-	2.0×10^{-16}
HÄSTHOLMEN						
HH1A1	Rapakivi granite (pyterlite)	2.2×10^{-19}	0.085	2.01×10^{-9}	1.71×10^{-12}	7.0×10^{-15}
HH1B	Rapakivi granite (pyterlite)					1.0×10^{-15}
HH1G	Rapakivi granite (pyterlite)					1.0×10^{-14}
HH1I1	Rapakivi granite (pyterlite)	1.0×10^{-18}	0.18	1.34×10^{-8}	2.41×10^{-11}	5.0×10^{-15}
HH1D1	Rapakivi granite (viborgite)	1.5×10^{-17}	0.105	3.20×10^{-9}	3.36×10^{-12}	1.0×10^{-15}
HH1E	Rapakivi granite (viborgite)					8.0×10^{-16}
HH1F1	Rapakivi granite (viborgite)	4.0×10^{-19}	0.065	1.60×10^{-9}	1.04×10^{-12}	2.0×10^{-15}
HH1N	Rapakivi granite (viborgite)					1.0×10^{-15}

Note: The sample RO2JK is made by putting the samples RO2J1 and RO2K2 together.

The sample RO2O2 was impermeable both in the through-diffusion and the permeability measurements. It was impermeable even under a pressure difference of about 100 kPa.

It is evident that the channel-flow results (the product $\varepsilon_p \times D_e$) are in each case smaller than the corresponding results obtained from the through-diffusion measurements. On the other hand, both the through-diffusion and permeability results are mutually consistent for all short samples. The biggest differences between the through-diffusion and channel-flow results are in the granite samples from Olkiluoto and the porphyritic granite samples from Kivetty. On the other hand, the corresponding results for the amfibolite samples from Romuvaara differ only about one decade. The both original amfibolite samples (RO2J1 and RO2K2) were measured separately and also by putting them together (RO2JK). The results were not consistent between these measurements. A possible reason for this discrepancy will be explained later on in this report.

Comparing the products $\varepsilon_p \times D_e$ between through-diffusion and channel-flow methods it is evident that the products $\varepsilon_p \times D_e$ between these two methods correlates best when the through-diffusion results are about 10^{-13} m^2/s. These small through-diffusion results indicate both that there are no microcracks in these short drill core samples and that the through-diffusion measuring times are long ones (more than about 1000 minutes) for short drill core samples. The permeability results indicate also that there are no microcracks in these samples. However, if the through-diffusion results are about 10^{-11} m^2/s and the corresponding permeability results are about 10^{-18} - 10^{-17} m^2, it is possible that there are microcracks in these samples. Furthermore, the through-diffusion measuring times are under 500 minutes for those short drill core samples (lengths about 20 mm). It is also very probable, that there are correspondingly microcracks in long drill core channel-flow samples. The mathematical model does not observe that helium penetrates through the long drill core samples in radial direction during the measurements and the fitted channel-flow results can be wrong (about 10^{-16} m^2/s, should be about 10^{-11} m^2/s). The same effect is seen from the results in Table 2, in which is shown all the channel-flow and the corresponding through-diffusion results measured by He-gas methods. Our earlier results are from the reports Hartikainen et al. 1996a and Hartikainen et al. 1997. In Table 2 is also shown results for Romuvaara and Hästholmen from our other study made for POSIVA during this year.

Table 2. *Porosities and effective diffusion coefficients for the channel-flow and through-diffusion samples from Olkiluoto, Kivetty, Romuvaara and Hästholmen. Diffusion coefficients are for helium in samples saturated by nitrogen gas ($D_e(He/N_2)$).*

Sample	Rock type	Through-diffusion ε_p [%]	Through-diffusion D_e [m²/s]	Through-diffusion $\varepsilon_p \times D_e$ [m²/s]	Channel-flow $\varepsilon_p \times D_e$ [m²/s]
OLKILUOTO					
OL-100	Mica gneiss (migmatitic)	0.018	1.05×10^{-10}	1.89×10^{-14}	1.00×10^{-15}
OL-101	Mica gneiss (migmatitic)	-	-	-	1.30×10^{-14}
OL-102	Mica gneiss (migmatitic)	0.075	2.3×10^{-10}	1.73×10^{-13}	7.00×10^{-16}
OL-103	Mica gneiss (migmatitic)	-	-	-	6.00×10^{-14}
OL-104	Mica gneiss (migmatitic)	2.2	3.20×10^{-10}	7.04×10^{-12}	2.50×10^{-13}
OL-206	Granite	0.12	5.20×10^{-9}	6.24×10^{-12}	2.70×10^{-13}
OL-207	Granite	0.11	4.60×10^{-9}	5.06×10^{-12}	3.00×10^{-14}
OL-208	Granite	0.09	6.55×10^{-9}	5.90×10^{-12}	2.00×10^{-14}
OL-209	Granite	-	-	-	8.00×10^{-14}
OL-210	Tonalite	0.28	7.00×10^{-10}	1.96×10^{-12}	2.70×10^{-13}
OL-211	Tonalite	0.07	4.40×10^{-10}	3.08×10^{-13}	1.60×10^{-13}
OL-212	Tonalite	-	-	-	1.00×10^{-13}
OL-213	Tonalite (slice 1)	0.07	6.60×10^{-10}	4.62×10^{-13}	1.60×10^{-13}
	(slice 2)	0.09	2.80×10^{-10}	2.52×10^{-13}	
Slice 1 is from the upper part and slice 2 from the lower part of the drill core sample.					
OL-214	Tonalite	-	-	-	1.00×10^{-14}
OL5A1	Granite	0.175	4.70×10^{-9}	8.23×10^{-12}	9.0×10^{-15}
OL5F1	Granite	0.20	1.85×10^{-8}	3.70×10^{-11}	1.0×10^{-15}
OL5E1	Mica gneiss	0.17	1.50×10^{-9}	2.55×10^{-12}	1.0×10^{-14}
OL5G1	Mica gneiss	0.053	5.00×10^{-10}	2.65×10^{-13}	4.0×10^{-14}
OL5B1	Tonalite	0.04	2.80×10^{-9}	1.12×10^{-12}	1.0×10^{-14}
OL5I1	Tonalite	0.17	1.23×10^{-9}	2.09×10^{-12}	1.0×10^{-14}
KIVETTY					
Ki-416	Porphyritic granodiorite *	0.085	7.80×10^{-9}	6.63×10^{-12}	3.00×10^{-13}
Ki-419	Porphyritic granodiorite *	0.03	3.10×10^{-9}	9.30×10^{-13}	2.20×10^{-13}
Ki-420	Porphyritic granodiorite *	0.04	9.40×10^{-10}	3.76×10^{-13}	2.00×10^{-13}
Ki-422	Porphyritic granodiorite *	0.0475	1.70×10^{-9}	8.08×10^{-13}	2.00×10^{-13}
Ki-425	Porphyritic granodiorite *	-	-	-	1.00×10^{-14}
Ki-427	Porphyritic granodiorite *	-	-	-	4.00×10^{-14}
* partially monzonite					
Ki-429	Porphyritic granite	0.055	4.50×10^{-10}	2.48×10^{-13}	1.00×10^{-13}
Ki-430	Porphyritic granite	-	-	-	1.00×10^{-14}
Ki-432	Porphyritic granite	0.0775	9.90×10^{-10}	7.67×10^{-13}	3.00×10^{-14}
Ki-433	Porphyritic granite	0.2	2.90×10^{-9}	5.80×10^{-12}	5.00×10^{-13}
Ki-434	Porphyritic granite	0.11	4.10×10^{-9}	4.51×10^{-12}	2.10×10^{-15}
Ki3B1	Porphyritic granodiorite	0.10	3.60×10^{-9}	3.60×10^{-12}	5.0×10^{-15}
Ki3C1	Porphyritic granodiorite	0.063	1.38×10^{-9}	8.69×10^{-13}	5.0×10^{-15}
Ki3D1	Porphyritic granite	0.16	8.05×10^{-9}	1.29×10^{-11}	8.0×10^{-16}
Ki3E1	Porphyritic granite	0.19	1.67×10^{-8}	3.17×10^{-11}	1.0×10^{-15}

continue ...

ROMUVAARA						
Ro-136	Mica gneiss *		-	-	-	1.90×10^{-14}
Ro-137	Mica gneiss *	(slice 1)	0.15	9.85×10^{-9}	1.48×10^{-11}	2.50×10^{-16}
		(slice 2)	0.22	2.50×10^{-8}	5.50×10^{-11}	
Slice 1 is from the upper part and slice 2 from the lower part of the drill core sample.						
Ro-138	Mica gneiss *		0.12	6.00×10^{-10}	7.20×10^{-13}	2.80×10^{-15}
Ro-139	Mica gneiss *		0.2	1.30×10^{-8}	2.60×10^{-11}	1.05×10^{-15}
Ro-141	Mica gneiss *		-	-	-	6.00×10^{-15}
* migmatitic						
Ro-143	Leukotonalite (gneiss)		-	-	-	1.00×10^{-14}
Ro-144	Leukotonalite (gneiss)		0.11	2.20×10^{-9}	2.42×10^{-12}	4.00×10^{-16}
Ro-147	Leukotonalite (gneiss)		0.17	2.40×10^{-9}	4.08×10^{-12}	2.80×10^{-15}
Ro-148	Leukotonalite (gneiss)		0.1	2.20×10^{-9}	2.20×10^{-12}	5.00×10^{-13}
Ro-149	Leukotonalite (gneiss)		0.23	2.15×10^{-9}	4.95×10^{-12}	9.20×10^{-13}
Ro-150	Granodiorite		0.12	3.60×10^{-9}	4.32×10^{-12}	3.50×10^{-15}
Ro-151	Granodiorite		-	-	-	7.00×10^{-15}
Ro-152	Granodiorite		0.055	1.13×10^{-9}	6.22×10^{-13}	1.20×10^{-13}
Ro-153	Granodiorite		-	-	-	1.00×10^{-13}
Ro-154	Granodiorite		0.1	3.00×10^{-9}	3.00×10^{-12}	2.00×10^{-12}
RO2A1	Leukotonalite (gneiss)		0.12	1.13×10^{-9}	1.36×10^{-12}	4.5×10^{-15}
RO2C1	Leukotonalite (gneiss)		0.19	8.50×10^{-9}	1.62×10^{-11}	7.0×10^{-15}
RO2J1	Amfibolite (A)		0.065	4.30×10^{-10}	2.80×10^{-13}	4.0×10^{-14}
RO2K2	Amfibolite (B)		0.14	1.88×10^{-9}	2.63×10^{-12}	2.0×10^{-13}
RO2JK	Amfibolite (A+B)					4.0×10^{-15}
RO2M1	Granodiorite		0.18	9.00×10^{-9}	1.62×10^{-11}	6.0×10^{-15}
RO2O2	Granodiorite		-	-	-	2.0×10^{-16}
RO2E	Migmatitic leukotonalite gneiss		0.18	8.50×10^{-9}	1.53×10^{-11}	2.0×10^{-14}
RO2F	Migmatitic leukotonalite gneiss		0.20	1.24×10^{-8}	2.48×10^{-11}	5.0×10^{-16}
RO2G	Migmatitic leukotonalite gneiss		0.16	1.43×10^{-8}	2.29×10^{-11}	2.0×10^{-16}
RO2H	Migmatitic leukotonalite gneiss		0.13	5.60×10^{-9}	7.28×10^{-12}	5.0×10^{-15}
RO2I	Migmatitic leukotonalite gneiss		0.14	5.60×10^{-9}	7.84×10^{-12}	4.0×10^{-15}
HÄSTHOLMEN						
HH1A1	Rapakivi granite (pyterlite)		0.085	2.01×10^{-9}	1.71×10^{-12}	7.0×10^{-15}
HH1B	Rapakivi granite (pyterlite)					1.0×10^{-15}
HH1G	Rapakivi granite (pyterlite)					1.0×10^{-14}
HH1I1	Rapakivi granite (pyterlite)		0.18	1.34×10^{-8}	2.41×10^{-11}	5.0×10^{-15}
HH1D1	Rapakivi granite (viborgite)		0.105	3.20×10^{-9}	3.36×10^{-12}	1.0×10^{-15}
HH1E	Rapakivi granite (viborgite)					8.0×10^{-16}
HH1F1	Rapakivi granite (viborgite)		0.065	1.60×10^{-9}	1.04×10^{-12}	2.0×10^{-15}
HH1N	Rapakivi granite (viborgite)					1.0×10^{-15}
HH1K	Rapakivi granite		0.15	2.20×10^{-9}	3.30×10^{-12}	5.0×10^{-15}
HH1M	Rapakivi granite		0.07	1.52×10^{-9}	1.06×10^{-12}	6.0×10^{-15}
HH1O	Rapakivi granite		0.12	4.00×10^{-9}	4.80×10^{-12}	8.0×10^{-15}
HH2A	Rapakivi granite		0.12	2.00×10^{-10}	2.40×10^{-13}	7.0×10^{-14}
HH2C	Rapakivi granite		0.17	3.30×10^{-9}	5.61×10^{-12}	1.0×10^{-14}

The reason for the discrepancy of amfibolite results can be the same as assumed above, i.e. the helium has penetrated through the long drill core sample (RO2JK) in radial direction during the channel-flow measurement. It is also evident from the results in Table 2, that there are often significant variations in both the through-diffusion and channel-flow products $\varepsilon_p \times D_e$ even within a given rock type from one site.

In this study the samples were cored from other holes than in our earlier studies, which must be emphasised. Furthermore, in this study the results for samples from Hästholmen were determined for the first time. These results are very comparable with those measured from the other possible repository sites by He-gas methods. The variations for the all results are shown in Table 3.

Table 3. *The variations for all the results as a function of rock type from Olkiluoto, Kivetty, Romuvaara and Hästholmen. The symbol* **N** *is the number of measured samples.*

Rock type	Through-diffusion				Channel-flow	
	N	ε_p	D_e	$\varepsilon_p \times D_e$	**N**	$\varepsilon_p \times D_e$
	[pcs]	[-]	[-]	[-]	[pcs]	[-]
OLKILUOTO						
Mica gneiss (migmatitic)	3	122	3	373	5	357
Mica gneiss	2	3	3	10	2	4
Granite	5	2	4	7	6	270
Tonalite	6	7	10	8	7	27
KIVETTY						
Porphyritic granodiorite partially monzonite	4	3	8	18	6	30
Porphyritic granodiorite	2	2	3	4	2	1
Porphyritic granite	6	3	37	128	7	625
ROMUVAARA						
Mica gneiss migmatitic	4	2	42	76	5	76
Leukotonalite (gneiss)	6	2	8	12	7	25
Migmatitic leukotonalite gneiss	5	2	3	3	5	100
Granodiorite	4	3	8	26	7	10000
Amfibolite	2	2	4	9	2	5
HÄSTHOLMEN						
Rapakivi granite (pyterlite)	2	2	7	14	4	10
Rapakivi granite (viborgite)	2	2	2	3	4	3
Rapakivi granite	5	2	20	23	5	14

The numbers shown in Table 3 have been calculated so, that the maximum value for each parameter of each rock type from the four possible repository sites has been divided by the minimum value. The number of measured samples **N** is so small in many cases, that very reliable conclusions are not possible to make. However, variations in porosity results are maximum 7 (tonalite from Olkiluoto) in one rock type of each site, except in case of mica gneiss (migmatitic) from Olkiluoto. The reason for this discrepancy is the Sample OL-104 (Table 2); there is a volume of clay in one corner of the sample and so the mesured porosity was high (2.2 %). Neglecting this porosity result, the variation in this rock type (migmatitic mica gneiss) is four. Variations of effective diffusion coefficient results are maximum 42 (migmatitic mica gneiss from Romuvaara) in one rock type of each site. Variations of porphyritic granite from Kivetty, rapakivi granite from Hästholmen and tonalite from Olkiluoto results are also more than one decade. Variations of the product $\varepsilon_p \times D_e$ results are essentially bigger both in through-diffusion and channel-flow methods comparing them to the porosity and the effective diffusion coefficient variations. Especially in the case of granodiorite from Romuvaara the channel-flow variation is 10000. The through-diffusion variations for the product $\varepsilon_p \times D_e$ results are more than one decade in 9 rock types of totally 15 rock types. Corresponding channel-flow variations are more than one decade in 11 rock types. The used mathematical model mentioned above has possibly caused some of these channel-flow result variations.

Porosities and migration properties have been measured from 9 to 21 through-diffusion samples (2 to 7 samples of each rock type) and from 13 to 26 channel-flow samples (2 to 7 samples of each rock type) from each possible repository sites. Totally 68 short through-diffusion samples and 74 long channel-flow samples have been measured. The data of analysed migration properties should be fulfilled to get more representative values of each site. More samples of each rock type ought to be measured by both through-diffusion and channel-flow methods to present more precise conclusions of determined migration properties.

5 CONCLUSIONS

It is shown here that the determined migration properties for the samples from Hästholmen are very comparable to those determined from the other three possible repository sites.

In this study it is also verified that the channel-flow results for the product $\varepsilon_p \times D_e$ results are in every case smaller than corresponding through-diffusion results. This difference is significant if the product $\varepsilon_p \times D_e$ for through-diffusion result is about 10^{-11} m^2/s. That indicates that there can be microcracks in these rock types and that the through-diffusion measuring times are under 500 minutes for the short drill core samples (lengths about 20 mm). The mathematical model for channel-flow measurements does not observe that helium penetrates through the long drill core samples in radial direction during the measurements and the fitted channel-flow results can be wrong (about 10^{-16} m^2/s, should be about 10^{-11} m^2/s). If the determined channel-flow results for the product $\varepsilon_p \times D_e$ is about 10^{-16} m^2/s, the through-diffusion measurement has to be made for the short drill core sample or samples cut from the long drill core sample to verify the consistency of the results. Further studies are clearly needed to analyse this phenomenon and to develop the channel-flow method in future.

Furthermore, the results show that in many cases there are significant variations in the product of porosity and diffusion coefficient even within a given rock type from one site.

It has also been shown once again, that the effective diffusion coefficients and permeability coefficients are well correlated. This indicates that these quantities are closely related, i.e. that the dominating migration pathways in diffusion and pressure induced flow are very similar.

Once again, it is also worth noting that there was one short drill core sample that was impermeable to gas in both the through-diffusion and the permeability measurements. The sample was impermeable even under a pressure difference of about 100 kPa. This may indicate that it has become (partly) saturated by some fluid possibly during the drilling. It is therefore important that more attention is paid to the careful handling of samples during the drilling in the future.

REFERENCES

Hartikainen, J., Hartikainen, K., Pietarila, H. & Timonen, J. 1995a. Permeability and diffusivity measurements with the He-gas method of disturbed zone in rock samples cored from the full-scale experimental deposition holes in the TVO Research Tunnel. Helsinki. Nuclear Waste Commission of Finnish Power Companies. Report YJT-95-16. 20 p. + app. 18 p. ISSN-0359-548X.

Hartikainen, J., Hartikainen, K., Hautojärvi, A., Kuoppamäki, K. & Timonen, J. 1996a. Helium gas methods for rock characteristics and matrix diffusion. Helsinki. Posiva Oy. Report POSIVA-96-22. 58 p. + app. 13 p. ISBN 951-652-021-9.

Hartikainen, J., Hartikainen, K. & Timonen, J. 1997. Through-diffusion, permeability, channel-flow and *in situ* results for porosity and migration properties of rock samples by He-gas methods. Helsinki. Posiva Oy. Report POSIVA-97-xx. xx p. + app. xx p. ISBN 951-652-xxx-x (to be published).

Hartikainen, K., Väätäinen, K., Hautojärvi, A. & Timonen, J. 1994a. Further development and studies of gas methods in matrix diffusion. In: Barkatt, A. & Van Konynenburg, R. (eds). Scientific Basis for Nuclear Waste Management XVII. Boston, USA. 1994. MRS Vol. 333. Pittsburgh. MRS. Pp. 821-826.

Hartikainen, K., Timonen, J., Väätäinen, K., Pietarila, H. & Hautojärvi, A. 1994b. Studies of matrix diffusion in gas phase (in Finnish). Helsinki. Nuclear Waste Commission of Finnish Power Companies. Report YJT-94-07. 27 p. + app. 2 p. ISSN-0359-548X.

Hartikainen, K., Hautojärvi, A., Pietarila, H. & Timonen, J. 1995b. Diffusion measurements on crystalline rock matrix. In: Murakami, T. & Ewing, R. (eds). Scientific Basis for Nuclear Waste Management XVIII. Boston, USA. 1995. MRS Vol. 353. Pittsburgh. MRS. Pp. 435-440.

Hartikainen, K., Pietarila, H., Rasilainen, K., Nordman, H., Ruskeeniemi, T., Hölttä, P., Siitari-Kauppi M. & Timonen, J. 1996b. Characterization of the altered zone around a fracture in Palmottu natural analogue. In: Murphy, W. & Knecht, D. (eds). Scientific Basis for Nuclear Waste Management XIX. Boston, USA. 1996. MRS Vol. 412. Pittsburgh. MRS. Pp. 839-846.

Väätäinen, K., Timonen, J. & Hautojärvi, A. 1993. Development of a gas method for migration studies in fractured and porous media. In: Interrante, C. & Pabalan, R. (eds). Scientific basis for nuclear waste management XVI. Boston, USA. 1993. MRS Vol. 294. Pittsburgh. MRS. Pp. 851-856.

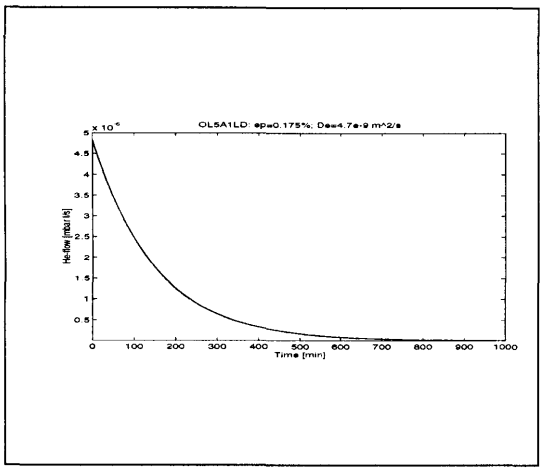

Figure 1. *Measured and fitted breakthrough curves for the sample OL5A1.*

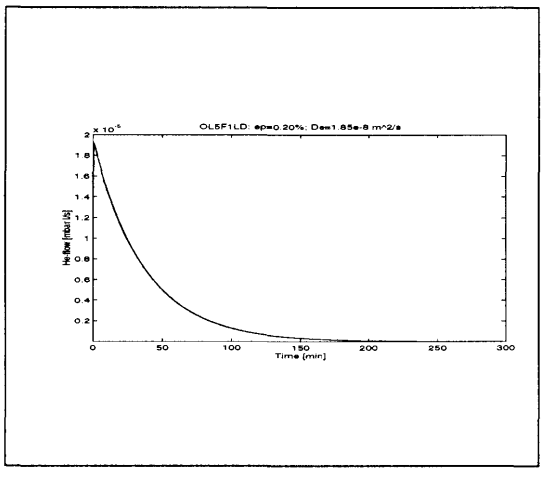

Figure 2. *Measured and fitted breakthrough curves for the sample OL5F1.*

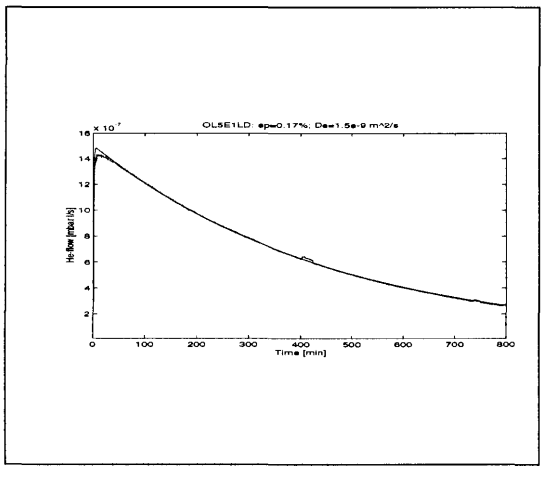

Figure 3. *Measured and fitted breakthrough curves for the sample OL5E1.*

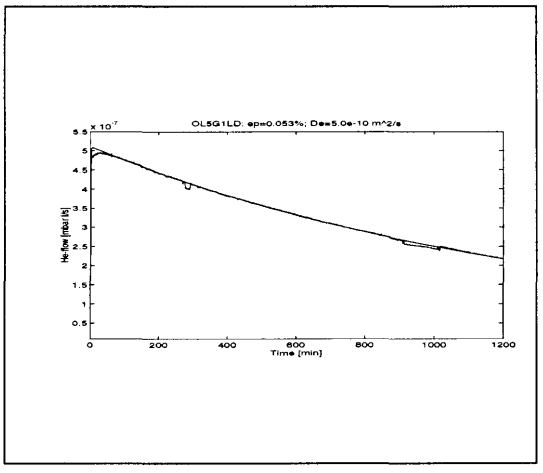

Figure 4. *Measured and fitted breakthrough curves for the sample OL5G1.*

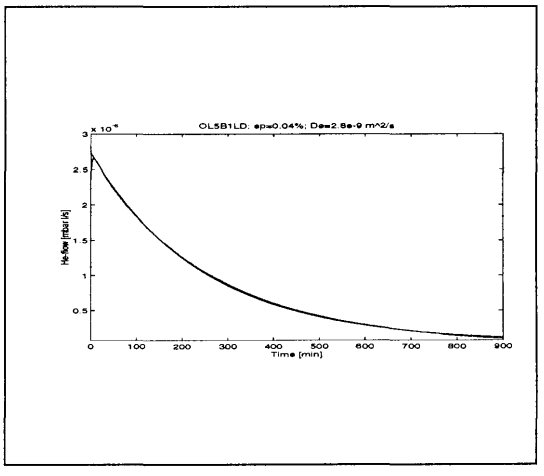

Figure 5. *Measured and fitted breakthrough curves for the sample OL5B1.*

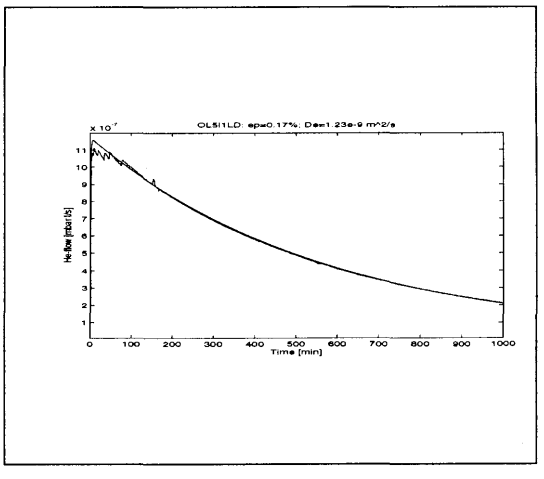

Figure 6. *Measured and fitted breakthrough curves for the sample OL5I1.*

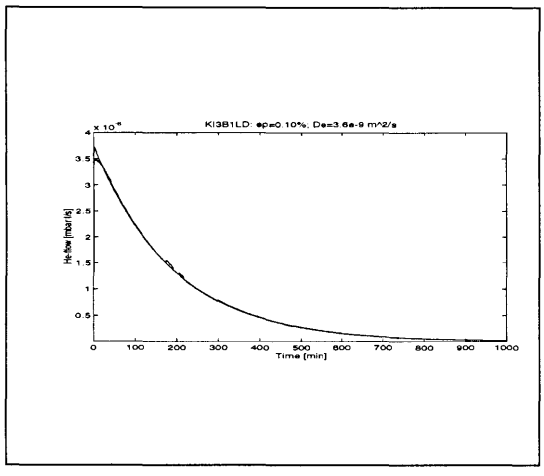

Figure 7. *Measured and fitted breakthrough curves for the sample Ki3B1.*

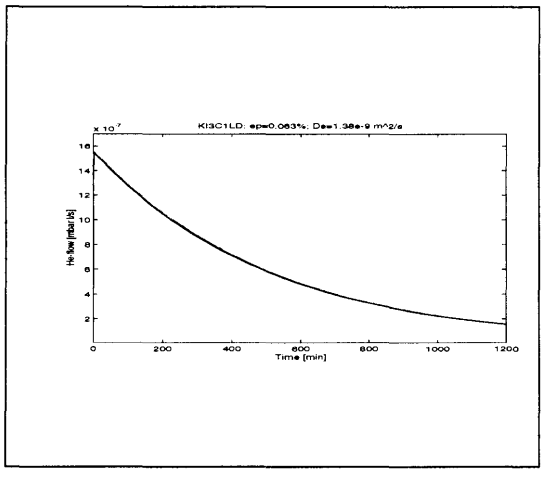

Figure 8. *Measured and fitted breakthrough curves for the sample Ki3C1.*

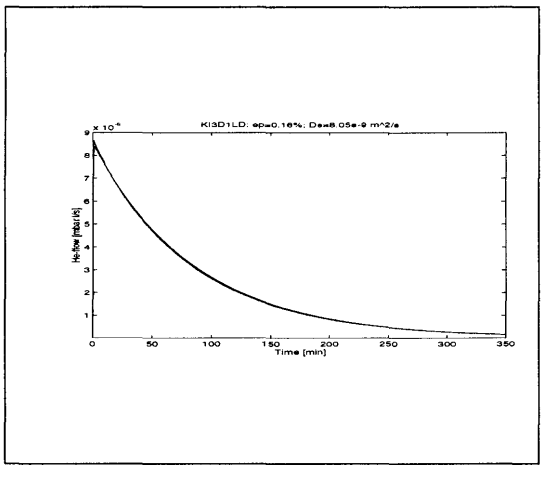

Figure 9. *Measured and fitted breakthrough curves for the sample Ki3D1.*

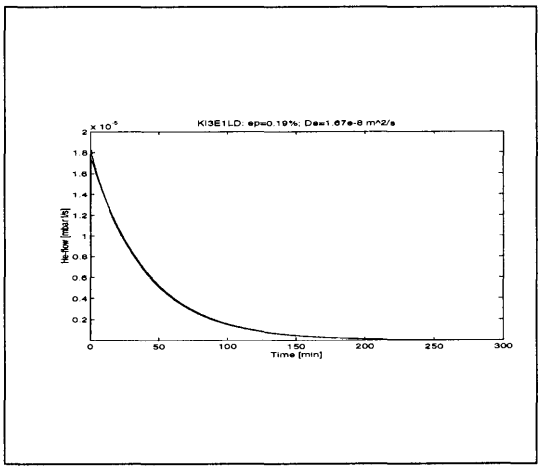

Figure 10. *Measured and fitted breakthrough curves for the sample Ki3E1.*

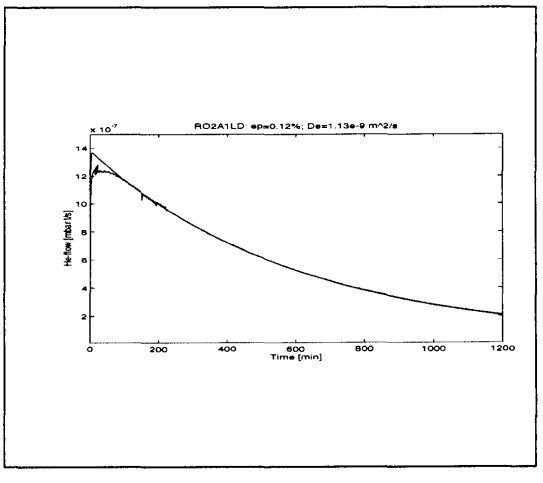

Figure 11. *Measured and fitted breakthrough curves for the sample RO2A1.*

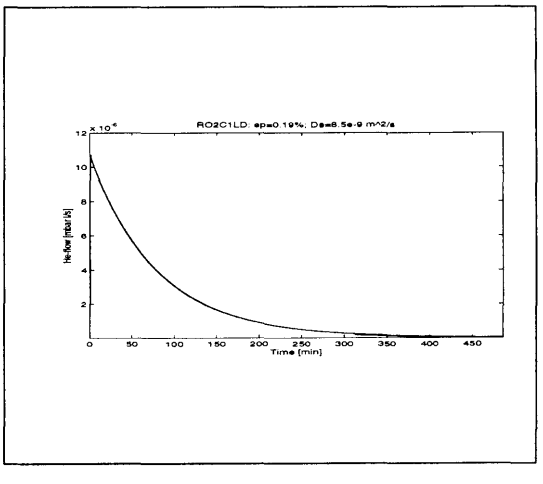

Figure 12. *Measured and fitted breakthrough curves for the sample RO2C1.*

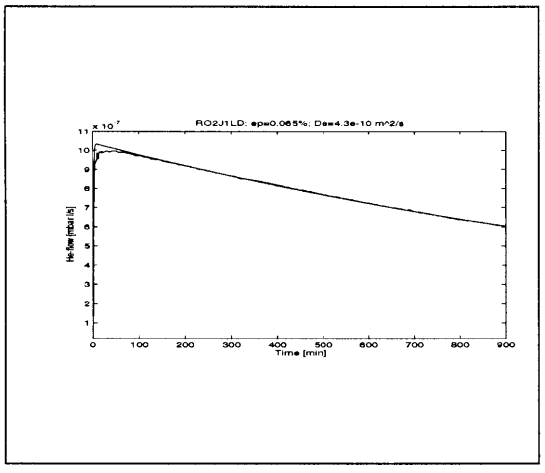

Figure 13. Measured and fitted breakthrough curves for the sample RO2J1.

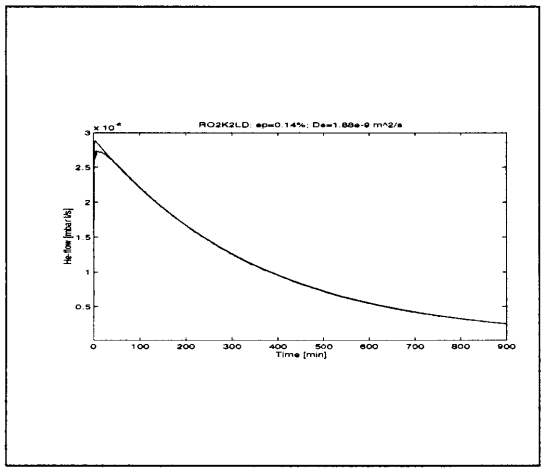

Figure 14. Measured and fitted breakthrough curves for the sample RO2K2.

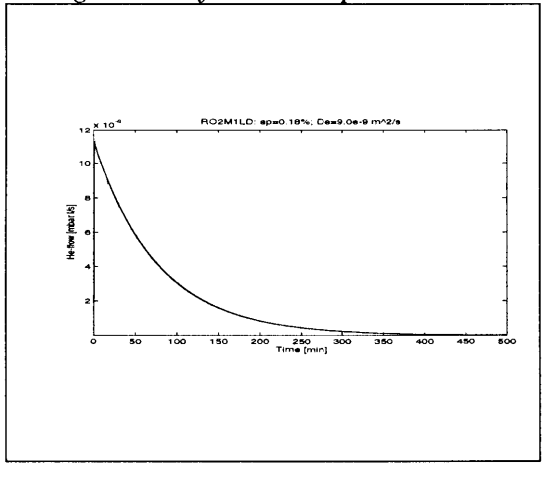

Figure 15. Measured and fitted breakthrough curves for the sample RO2M1.

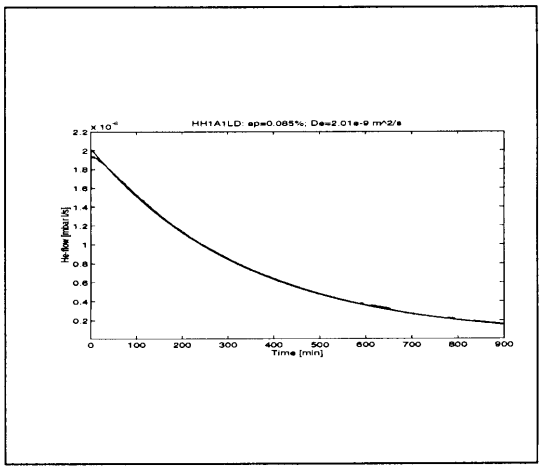

Figure 16. Measured and fitted breakthrough curves for the sample HH1A1.

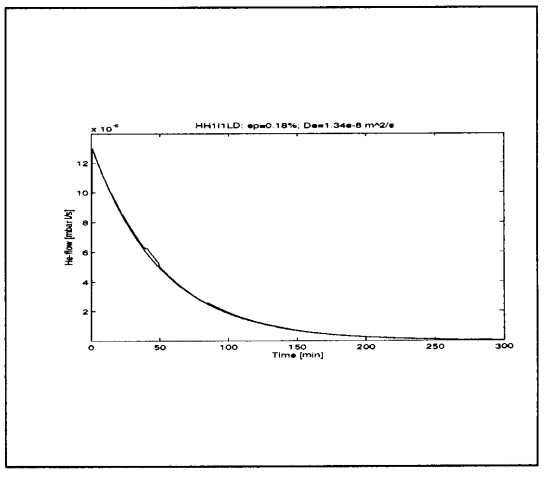

Figure 17. Measured and fitted breakthrough curves for the sample HH1I1.

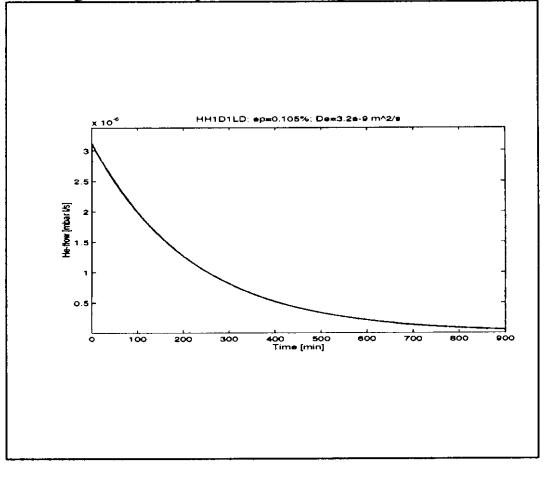

Figure 18. Measured and fitted breakthrough curves for the sample HH1D1.

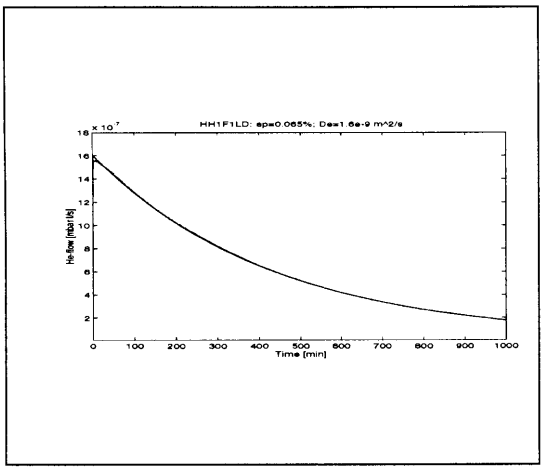

Figure 19. *Measured and fitted break-through curves for the sample HH1F1.*

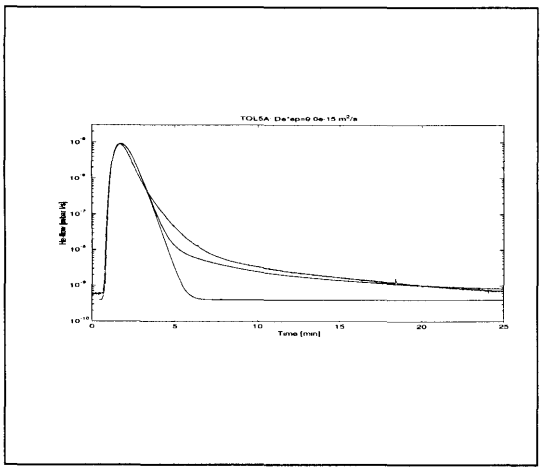

Figure 1. *Measured and fitted breakthrough curves for the sample OL5A.*

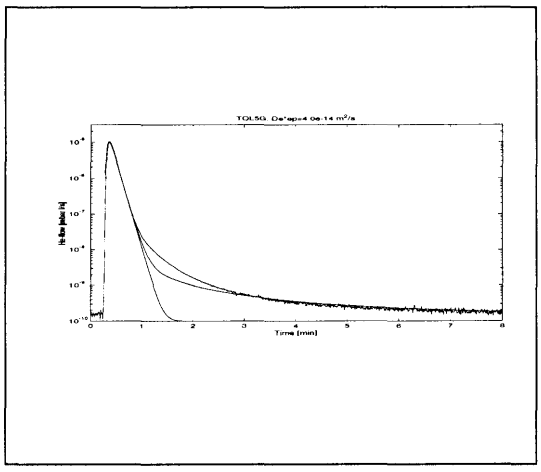

Figure 4. *Measured and fitted breakthrough curves for the sample OL5G.*

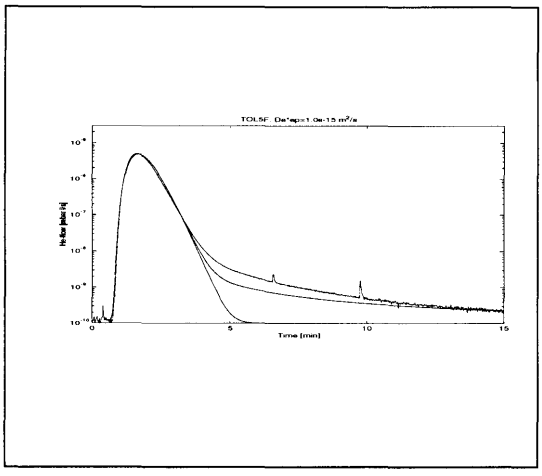

Figure 2. *Measured and fitted breakthrough curves for the sample OL5F.*

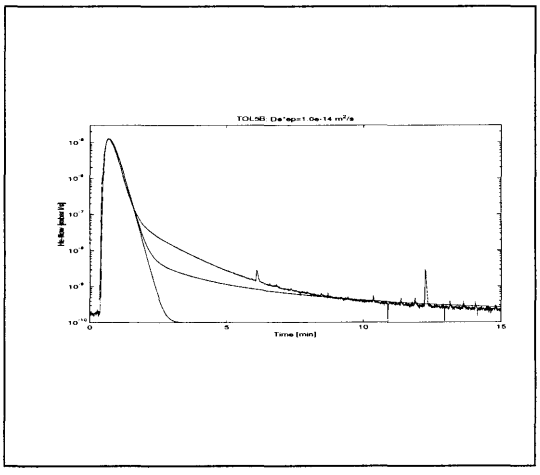

Figure 5. *Measured and fitted breakthrough curves for the sample OL5B.*

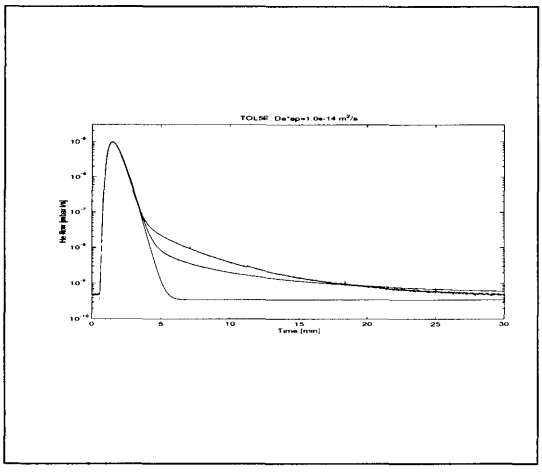

Figure 3. *Measured and fitted breakthrough curves for the sample OL5E.*

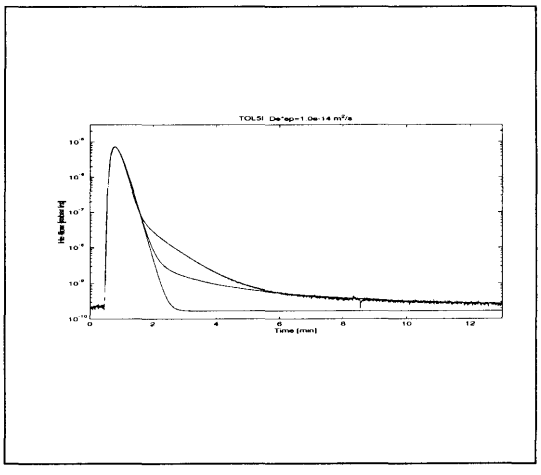

Figure 6. *Measured and fitted breakthrough curves for the sample OL5I.*

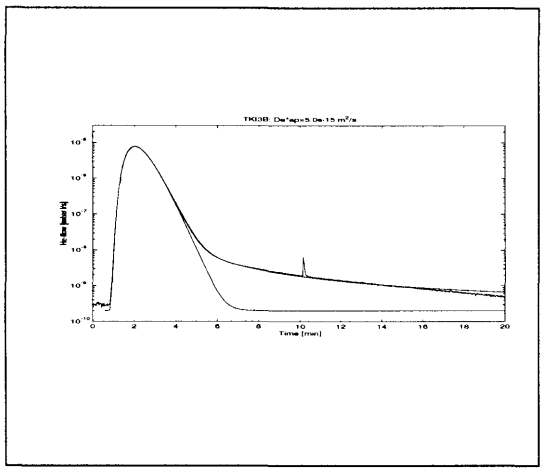

Figure 7. *Measured and fitted breakthrough curves for the sample Ki3B.*

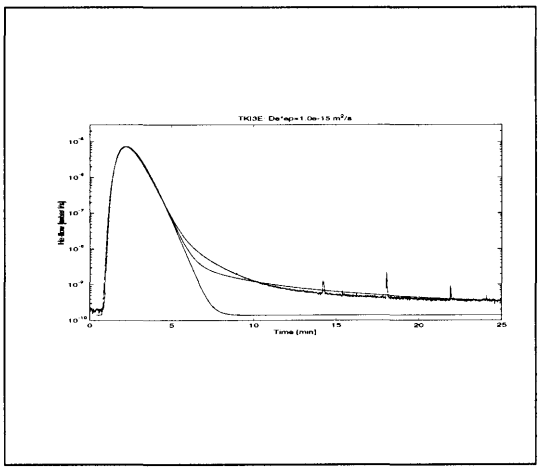

Figure 10. *Measured and fitted breakthrough curves for the sample Ki3E.*

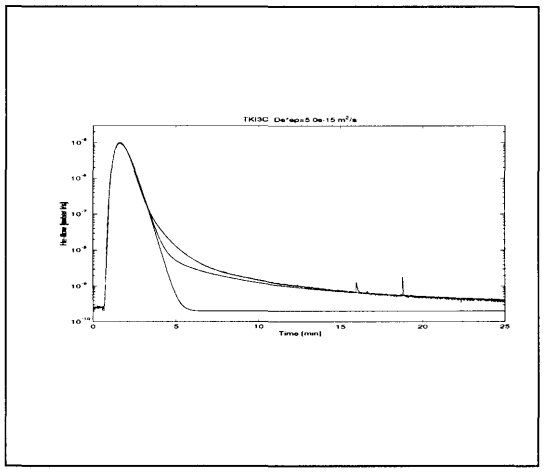

Figure 8. *Measured and fitted breakthrough curves for the sample Ki3C.*

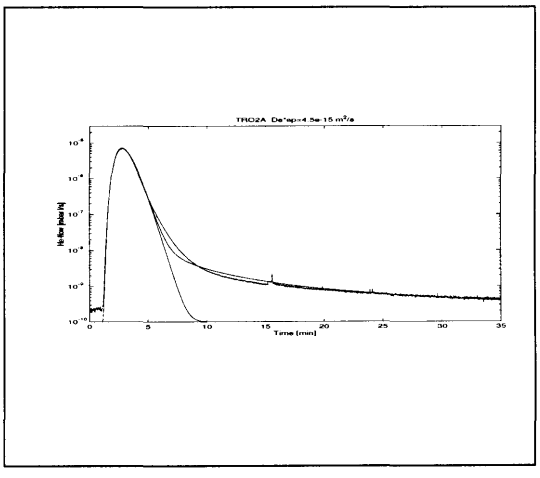

Figure 11. *Measured and fitted breakthrough curves for the sample RO2A.*

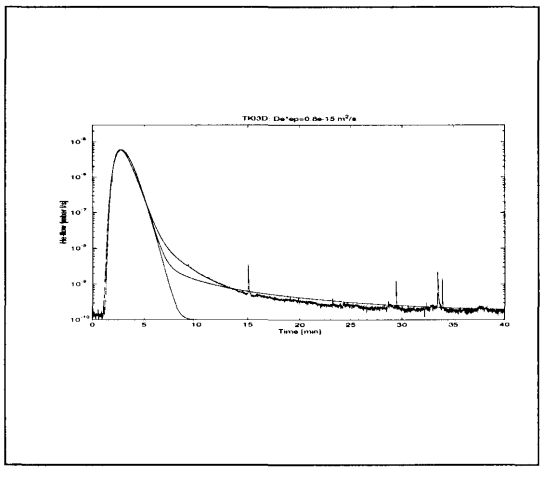

Figure 9. *Measured and fitted breakthrough curves for the sample Ki3D.*

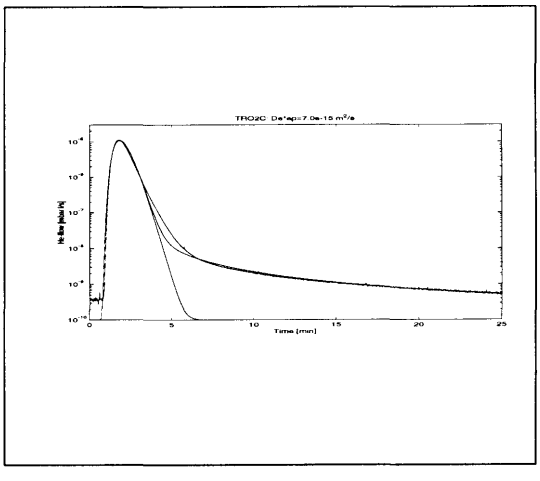

Figure 12. *Measured and fitted breakthrough curves for the sample RO2C.*

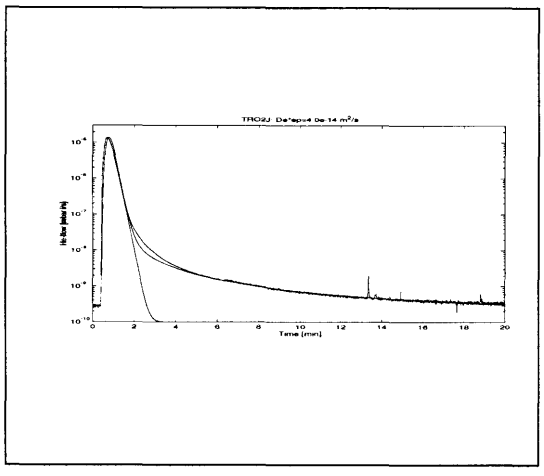

Figure 13. Measured and fitted breakthrough curves for the sample RO2J.

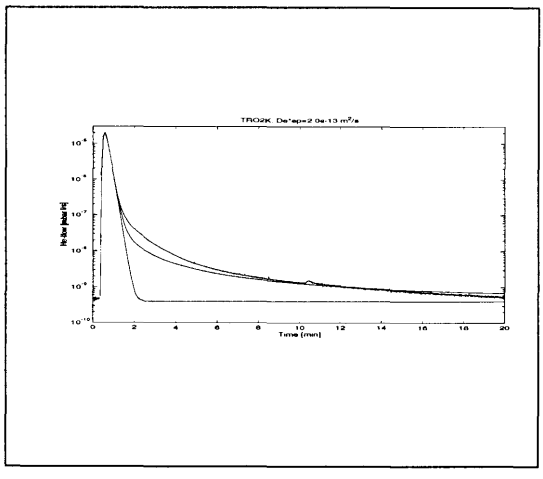

Figure 14. Measured and fitted breakthrough curves for the sample RO2K.

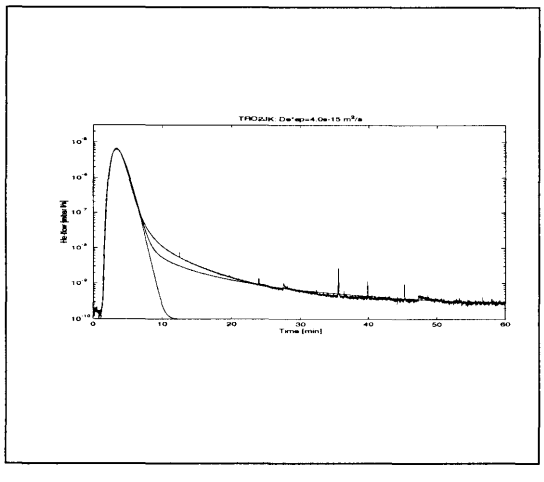

Figure 15. Measured and fitted breakthrough curves for the sample RO2JK.

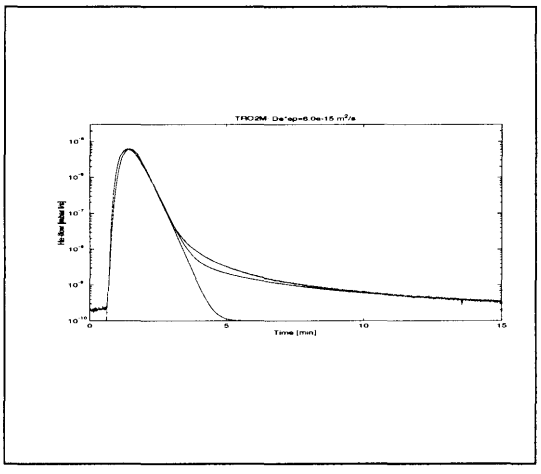

Figure 16. Measured and fitted breakthrough curves for the sample RO2M1.

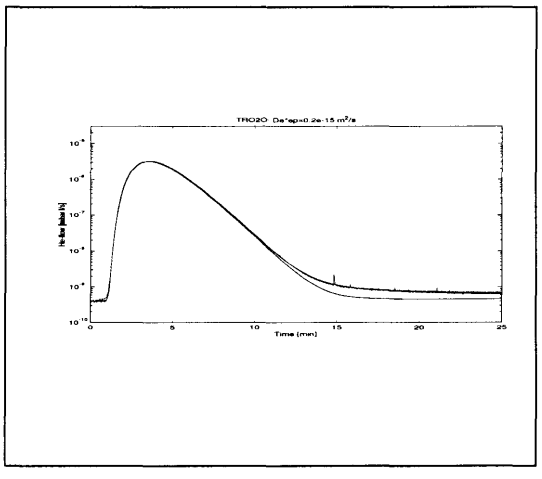

Figure 17. Measured and fitted breakthrough curves for the sample RO2O2.

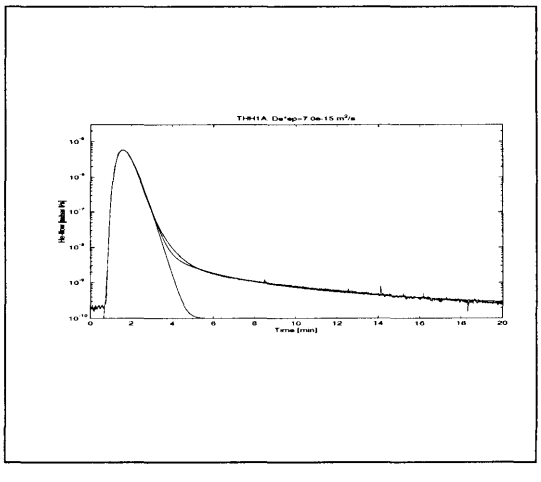

Figure 18. Measured and fitted breakthrough curves for the sample HH1A.

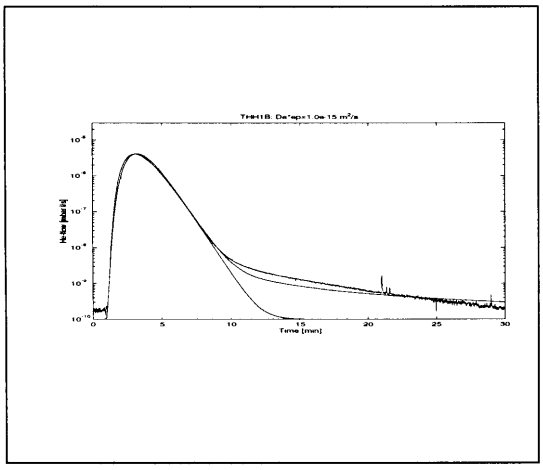

Figure 19. *Measured and fitted breakthrough curves for the sample HH1B.*

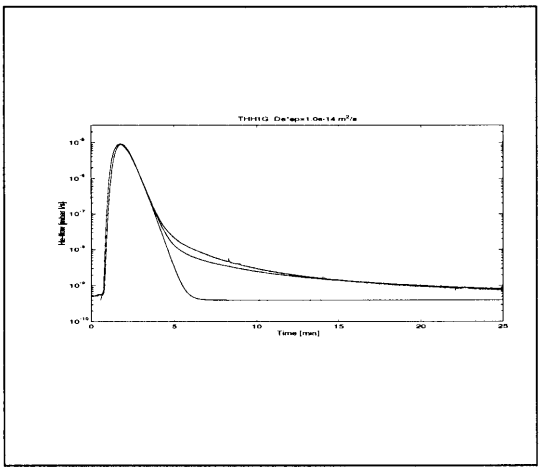

Figure 20. *Measured and fitted breakthrough curves for the sample HH1G.*

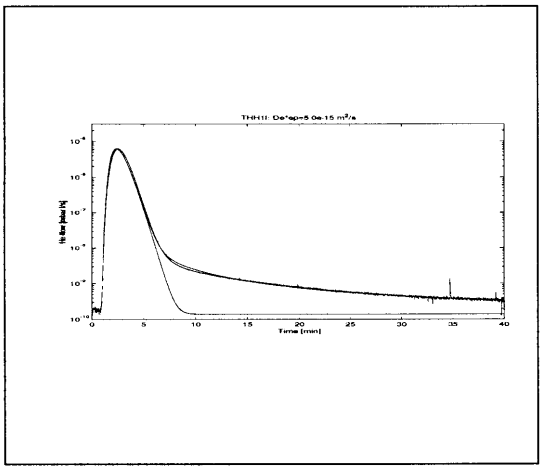

Figure 21. *Measured and fitted breakthrough curves for the sample HH1I.*

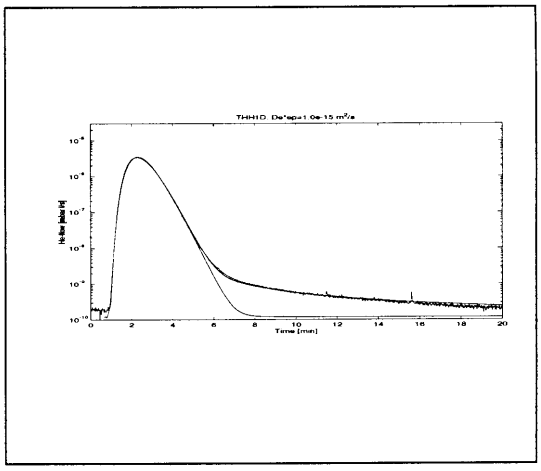

Figure 22. *Measured and fitted breakthrough curves for the sample HH1D.*

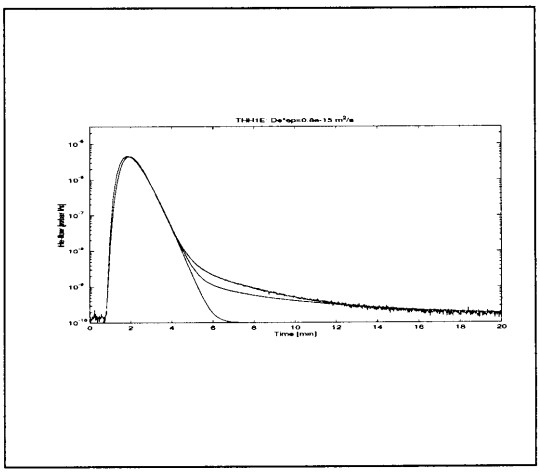

Figure 23. *Measured and fitted breakthrough curves for the sample HH1E.*

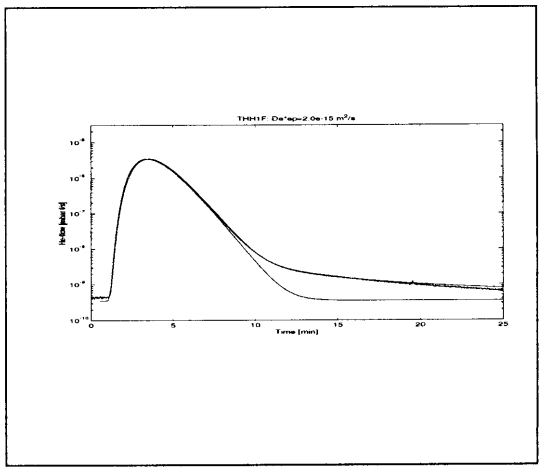

Figure 24. *Measured and fitted breakthrough curves for the sample HH1F.*

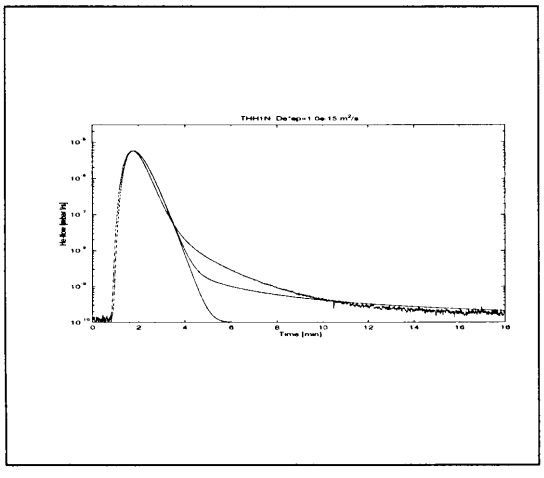

Figure 25. *Measured and fitted break-through curves for the sample HH1N.*